



Experimental investigation on heat transfer in horizontal-tube falling-film evaporator

Shengqiang Shen*, Xingsen Mu, Yong Yang, Gangtao Liang, Xiaohua Liu

Key Laboratory for Desalination of Liaoning Province, Dalian University of Technology, Dalian 116024, Liaoning, China, Tel. +86 411 84708464; Fax: +86 411 84707963; emails: zzbshen@dlut.edu.cn, magicruby@gmail.com (S. Shen)

Received 7 August 2013; Accepted 23 July 2014

ABSTRACT

An experimental platform for horizontal-tube falling-film evaporation was set up to measure heat transfer characteristics. Experiments were carried out to show how the heat transfer coefficient (HTC) was affected by different parameters including spray Reynolds number (Re), saturation temperature, salinity, and tube arrangement. The results revealed that the HTC increased first and then decreased with growth of Re, and the HTC of seawater decreased with increasing saturation temperature. The results also showed that the HTC of rotated square pitch was higher than triangular pitch, rotated triangular pitch, and square pitch, but the heat transfer capacity per unit volume of triangular pitch was the highest. Meanwhile, the HTC decreased during the increase of salinity.

Keywords: Desalination; Horizontal-tube falling-film evaporator; Tube arrangement; Salinity

1. Introduction

About 70% of the earth's surface is covered by water, and the oceans represent the earth's major water reservoir. However, about 97% of the earth's water is seawater while other 2% fresh water is locked in ice caps and glaciers. Available fresh water just accounts for less than 0.5% of the earth's total water reserves [1]. Furthermore, most of fresh water underlie the earth's surface, so it is too deep to access in an economically efficient manner. Additionally, seawater is unsuitable for human consumption and for industrial and agricultural using. By removing salt from the seawater with unlimited supply ability, desalination has been considered as an important source of fresh water.

Methods of desalination mainly include thermal desalination, membrane, and chemical desalination.

Although there are so many methods existed, among them most widely used are reverse osmosis, multistage flash distillation, and multiple effect distillation (MED). And low-temperature multiple effect desalination is selected as the main technology of desalination in the second generation dual-purpose power plant [2].

Falling-film evaporation on horizontal tubes is an effective design for evaporators with high heat transfer coefficient (HTC) at lower flow rates, low evaporation temperature, and small temperature differences. The liquid flowing outside heat transfer tubes helps the steam and liquid phase to be separated dispersedly, which makes the HTC relatively high. The falling-film evaporation on horizontal tubes is a preference for low-temperature multiple effect distillation (LT-MED) desalination plant which usually works below 70°C. As metal tubes cannot be corroded and scaled easily by seawater below 80°C, so less metal materials would be

*Corresponding author.

used and distillate cost can be reduced. Because of these characters, it is a dominant design for evaporators of MED in large-scale desalination plant.

Several experimental and theoretical studies on falling-film evaporation have been reported in published works. Most of them were carried out for refrigeration facilities. Zeng [3,4] made an experiment with ammonia as the evaporation liquid. The tube bundle was composed of stainless steel tubes of 19 mm diameter. The saturation temperature test range was from -23 to 10°C , and the heat flux ranged from 3.2 to 35 kW/m^2 . The paper concluded that the rotated square-pitch bundle tended to provide a higher HTC than triangular-pitch bundle at a low saturation temperature, and triangular-pitch bundle was more likely to provide a higher coefficient at a high saturation temperature. Moeykens and Pate [5] made an experiment with R-134a as the evaporation liquid, and the tube bundle was composed of copper tubes of 19 mm diameter. It was reported that the triangular-pitch bundle gave a higher bundle-averaged HTC than the rotated square-pitch bundle at heat flux of $0\text{--}35\text{ kW/m}^2$. Liu and Yi [6] and Ribatski and Jacobi [7] were also conducting similar research, and they had come to a similar conclusion. Although many studies have been done on influences of a tube bundle on a HTC, the research focused on desalination is still inadequate. In the present study, the experimental conditions are approximately identical to the actual operating conditions of a desalination plant, such as tube bundle, tube diameter, evaporation temperature, and seawater is used as the experimental fluid.

Yang and Shen [8] reported that the HTC of pure water was slightly higher than that of seawater by experiments in which the tubes were made of one kind of Al-brass with an outer diameter of 14 mm. The range of spray density was $0\text{--}0.062\text{ kg/ms}$, and the heat flux range was $5\text{--}30\text{ kW/m}^2$. Jelino [9] found a different result that the HTC of pure water was almost identical to the seawater. In the experiment, the Al-brass tube with a diameter of 50.8 mm was used. Both fresh water and seawater were taken as experimental liquids. The range of heat flux was $12\text{--}88\text{ kW/m}^2$, and the range of T_{sat} was $38\text{--}126^{\circ}\text{C}$. The different views of the effect of salinity on the HTC cause the interest to investigate this phenomenon further.

In order to further understand the heat transfer characteristics of horizontal-tube falling-film evaporation for seawater, the experimental devices were set up according to some deficiencies of previous research mentioned in the earlier paragraph, and the experimental research for some parameters influencing heat transfer of horizontal-tube falling-film evaporation was finished.

2. Experiment process

2.1. Experiment system

The photo of the experimental setup is shown in Fig. 1. The experiment system for horizontal-tube falling-film evaporation process is given in Fig. 2. An illustration of the experimental apparatus used in this investigation is presented in Fig. 3. The horizontal tube assembly is placed in the cylindrical casing which is equipped with front and back glass windows. The assembly consists of a feed tube, a heating tube, and four dummy tubes. The main function of the dummy tubes is to make the liquid film be uniformly distributed on the outer surface of the heating tube. The feed tube and dummy tubes were made of Al-brass with 25.4 mm outside diameter. The heating tube was made of Al-brass. The heating tube length is 2,000 mm with the effective length of 1,600 mm.

The electrical bar is used as the heating source, and the heat power is adjustable.

The experiments were carried out at different saturation temperatures, pressures, tube pitches, and different spray densities. The temperatures were measured by thermocouples. Calibration of thermocouples



Fig. 1. Photo of the experimental setup.

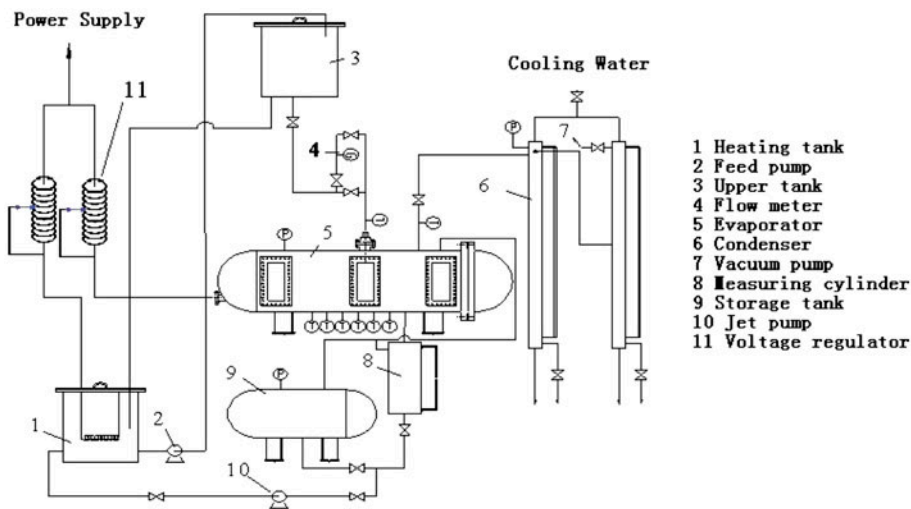


Fig. 2. Experimental system diagram.

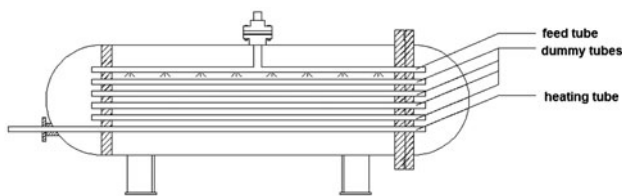


Fig. 3. The tube bundle in the evaporator.

was done before the experiment to maintain the maximum error less than 0.05°C . Five sets of thermocouples were arranged axially on the surface of the heating tube. The distance between the two sets of thermocouples was 350 mm. The thermocouple arrangement on the heating tube is shown in Fig. 4.

Pressure was measured by pressure sensors. The measuring range of the pressure sensor was from -0.1 to 0 MPa, and the precision was 0.2 kPa.

The spray densities were measured by a rotameter. The measuring range was 100 – $1,000$ L/h, and the precision was $\pm 1.5\%$. The spray tube was equipped with dripping holes. The hole diameter was 1.5 mm, hole

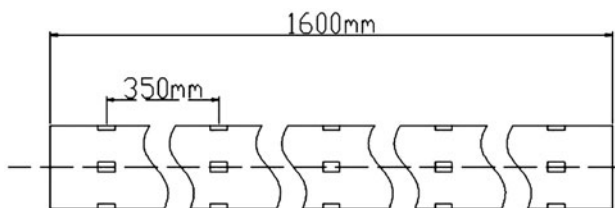


Fig. 4. Arrangement of thermocouples.

spacing was 20 mm, and 80 dripping holes at the bottom of spray tube were obtained by the Taylor instability equation [10]. The heating tube surface was completely wetted at Re number between 200 and 600 .

The measuring signal was collected by Henghe 2300, and the LabVIEW made data visual while saved.

The fluids used in the experiments were seawater, concentrated seawater, and low-salinity seawater, respectively. The seawater for the experiment was taken from the Yellow Sea near Dalian (a city at north-east China) with a salinity of 3.0% . The concentrated seawater was obtained from evaporation of seawater with 4.5% salinity. The low-salinity seawater was composed of pure water mixed with seawater.

More details were described in previous papers [11].

The uncertainty analysis is showed in Table 1.

2.2. Experiment process and method

The evaporator is the main equipment in this experiment. During the experiment process, a certain vacuum degree was fixed. A vacuum pump was used both at the initial state of the system for air extraction in the experimental system and process for discharging non-condensing gas produced during the experiment. All through the experiment at each measuring point, the working condition was sustained at a steady state for at least 20 min.

In the experiment process, feed water was heated to the saturation temperature corresponding to the pressure in the evaporator. Then, it was pumped to the upper tank where the water was kept at a fixed level. The feed water flowed at a steady rate by

Table 1
Experimental uncertainties

Position	Instrument	Accuracy
Feeding tube	Thermocouple	±0.05°C
	Rotameter	±1.5%
	Testo 240 Conductivity measuring instrument	±1 mg/L
Heating tube	Thermocouples	±0.05°C
	Power governor	±0.5%
Evaporator	Pressure sensors	±0.2 KPa
	Thermocouple	±0.05°C

gravity and the pressure difference outside and inside of the evaporator. It was sprayed well-distributed to the heating tube surface via spray tubes and dummy tubes; then, a liquid film was formed on the heating tube outer surface and dropped off continuously. The heat exchange between the liquid film and the heating tube surface converted part of the water into vapor. Then in the condensers, the vapor was condensed back to water again in order to sustain a certain degree of vacuum and to measure the evaporation capacity. The rest non-evaporated water was pumped back into the heating tank again for the next circulation.

Different vacuums corresponding to the evaporation temperature are chosen to simulate working conditions of different effect evaporators in an MED desalination plant. The influence of spray density on the evaporative HTC is also recorded by changing the feed water flow rate.

3. Experimental results and discussion

In the experiment, the heat flux q ranged from 0 to 24 kW/m². The saturation temperature was between 45 and 70°C, and the Re number was between 100 and 600, corresponding to a typical working range of an LT-MED desalination plant.

To calculate the HTC, the following formula is used.

$$h = \frac{Q_a}{F_a \Delta t} = \frac{q}{\Delta t} \quad (1)$$

In the experiment, F_a remained constant, Q_a was obtained by measuring the power of the heating tube, Δt was obtained by the thermocouples (1 thermocouple was located in the spray tube to get liquid temperature, and the others were distributed on the surface of the heating tube.), so h could be calculated.

To calculate the Reynolds number, the following formula is used.

$$Re = \frac{4\Gamma}{\eta} \quad (2)$$

3.1. Effect of the tube arrangement

Four most commonly used tube arrangements in a horizontal-tube falling-film evaporator are shown in Fig. 5. The relative tube pitch is normally taken 1.3. So the vertical tube spacing of rotated triangular pitch and square pitch is 33.02 mm, the triangular pitch is 57.2 mm, the rotated square pitch is 45.7 mm, respectively.

The relationship between the HTC and tube arrangements is shown in Figs. 5–7. The tube spacing is 33.02, 45.7 and 57.2 mm, separately. The saturation temperature is between 50 and 70°C (operating pressure 12.2–30.7 kPa), Re is between 150 and 550, the salinity is 30% (30 g/kg), and the q is 12 kW/m².

Results in Figs. 6–8 indicate that the HTC becomes higher during the increase of Re. When Re reaches about 400, the increase trend of the curve slows down. The reason is that when seawater drops reach the surface of the tube, the higher the flow rate, the stronger the liquid film disturbance, which will result in a higher HTC. However, the film thickness increases with Re. After Re reaches a certain value, the increasing liquid film thickness will hinder the

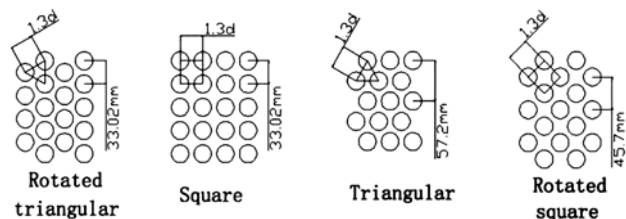


Fig. 5. Tube arrangements.

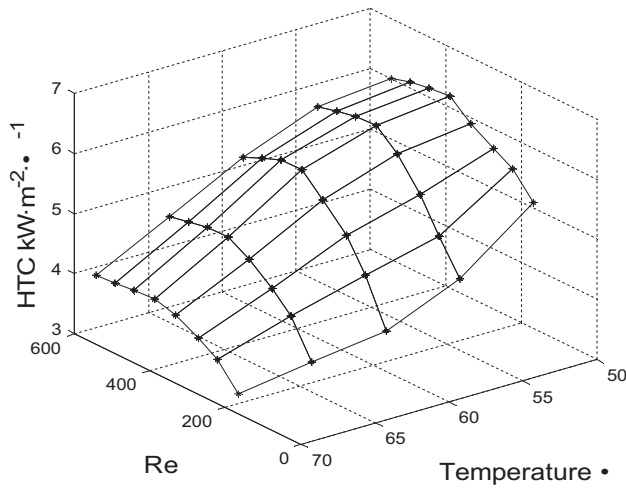


Fig. 6. Distribution of h at different Re and saturation temperature when the tube spacing is 33.02 mm.

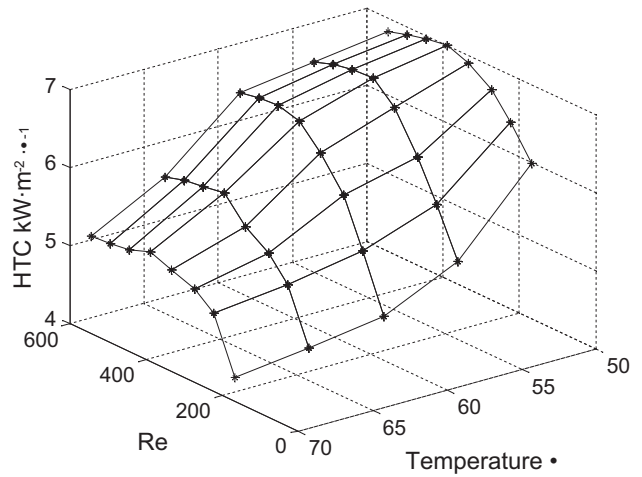


Fig. 8. Distribution of h at different Re and saturation temperature when the tube spacing is 57.2 mm.

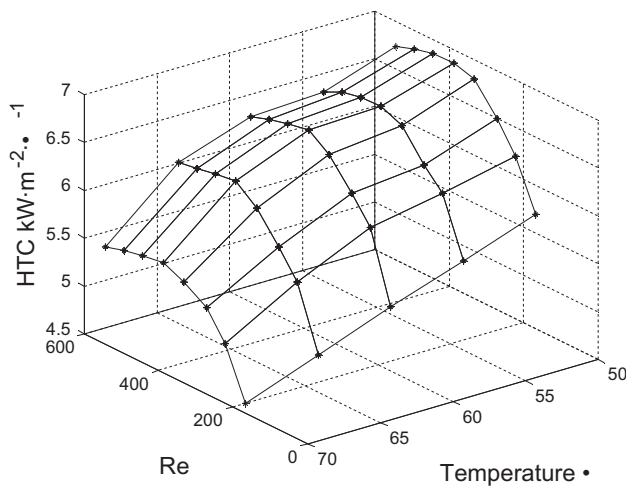


Fig. 7. Distribution of h at different Re and saturation temperature when the tube spacing is 45.7 mm.

growth of the HTC. In addition, the surface wetting is one of major reasons affecting the HTC, which decreases in low-Re conditions.

An interesting phenomenon shown in the figures is that the HTC becomes low during the increase of T_{sat} . It is different from the experimental fluid of fresh water [11], because the heat conduction λ of seawater decreases with T_{sat} (Table 2) [12]. Meanwhile, we can see from Fig. 9 [13] that the surface tension increases with T_{sat} in this experimental conditions (the evaporation temperature is 50–70 °C). There may be more than two reasons for this strange phenomenon.

It was also found that the HTC with the rotated square-pitch arrangement is the highest, followed by triangular-pitch, then square-pitch and rotated

Table 2

Thermal conductivity of seawater and fresh water

T_{sat} (°C)	λ of seawater (W/m°C)	λ of freshwater (W/m°C)
50	0.576	0.644
55	0.573	0.649
60	0.569	0.654
65	0.566	0.659
70	0.562	0.663

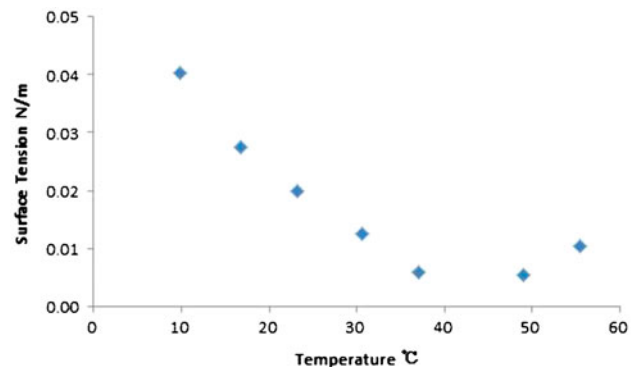


Fig. 9. Distribution of surface tension at different temperatures [13].

triangular-pitch arrangement. The reason is that droplet falls are caused by the gravity in the process of the falling film, so bigger tube spacing results in greater kinetic energy in the droplet when it comes into contact with the outer surface of the heating tube, and fluctuation in the film is intensified. So convection heat transfer is strengthened, which can lead to a higher HTC. However, when tube spacing is too large,

Table 3
n and some *h* of four tube arrangements

Tube arrangement	<i>n</i>	<i>h</i> (50°C, Re = 300)	<i>h</i> (60°C, Re = 300)	<i>h</i> (70°C, Re = 300)
Rotated square	1,764	6.819	6.456	5.558
Triangular	1,947	6.701	6.282	5.355
Rotated triangular	1,947	5.927	5.345	4.131
Square	900			

the droplet falls can produce more spatters of the liquid, which will reduce the actual Re.

When $D = 25.4$ mm, the amount of tubes in the unit cross-sectional area (1 m^2) and some h are given in Table 3.

The total heat transfer capacity is calculated by the following equation:

$$Q_a = hF_a \Delta t = hmF_s \Delta t \quad (3)$$

Due to fixed experimental conditions, F_s and Δt are constant, then the total heat transfer capacity in the unit cross-sectional area is determined by the product of n and h . Thus Φ is defined in this paper.

$$\Phi = \frac{Q_a}{F_s \Delta t} = hn \quad (4)$$

Φ is able to reflect the magnitude of the total heat transfer capacity in the unit cross-sectional area, so it can be used as a criteria to estimate the effective volume of the evaporators.

The n of triangular pitch is equal to that of rotated triangular pitch, and the h of triangular pitch is higher than that of rotated triangular pitch, so $\Phi_{\text{tri}} > \Phi_{\text{tri}}$. The $n_{\text{tri}} > n_{\text{squ}}$, and the $h_{\text{tri}} > h_{\text{squ}}$, so $\Phi_{\text{tri}} > \Phi_{\text{squ}}$. The $n_{\text{tri}} = 1,947$, $n_{\text{rsqu}} = 1,764$, $\frac{n_{\text{tri}}}{n_{\text{rsqu}}} = 1.10$, the n_{tri} is 10% higher than the n_{rsqu} , and the h_{rsqu} is higher than h_{tri} , but the difference is less than 10% through comparing Figs. 6 and 7, so $\Phi_{\text{tri}} > \Phi_{\text{rsqu}}$.

As a result, the triangular pitch has a higher value of Φ .

3.2. Effect of salinity

Figs. 10 and 11 show the comparison of h with three different salinities at the T_{sat} of 55°C and 60°C. The Re is between 150 and 550. It can be seen from the figures that h of different salinities has the same changing tendency, and all of them increases first, and then decreases during the increase of Re. Meanwhile, the h with salinity of 1.5% is the highest, the seawater is next, and salinity of 4.5% is the lowest. Due to the liquid viscosity becoming higher with the increase of S , [14] the

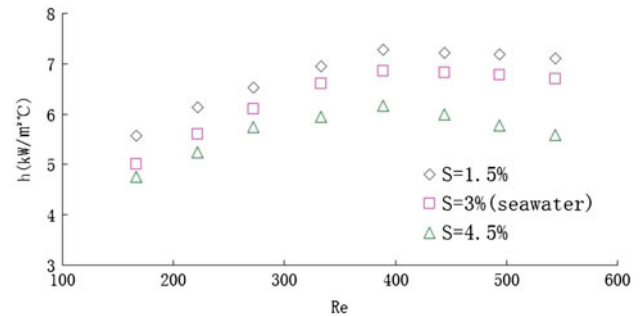


Fig. 10. Distribution of h at different Re and salinities when the saturation temperature is 55°C.

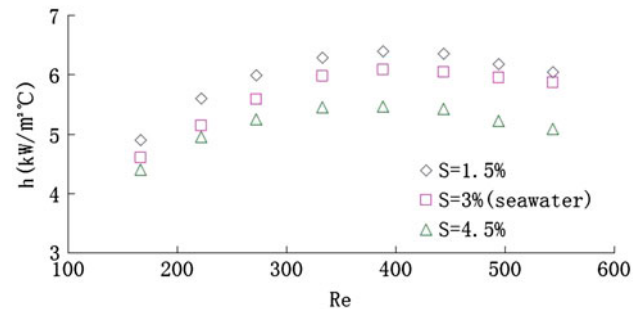


Fig. 11. Distribution of h at different Re and salinities when the saturation temperature is 65°C.

liquid film becomes thinner, and so does the thickness for the thermal boundary layer which can reduce thermal resistance. Besides, the heat conductivity decreases with the increase of S [12], it also reduces the thermal resistance of the liquid film. The surface tension of seawater becomes higher with the increase of S [14], so the liquid disturbance becomes weaker, and the convection heat transfer is deteriorated. All of the foregoing reasons will result in a lower h .

4. Conclusions

- (1) The heat transfer coefficient increases first and then decreases during the increase of Re.

- (2) The heat transfer coefficient of seawater becomes low during the increase of T_{sat} .
- (3) In the experimental conditions, the heat transfer coefficient of the rotated square pitch is the highest, followed by the triangular pitch, and the rotated triangular pitch and square pitch are the lowest.
- (4) The triangular pitch has a higher value of Φ .
- (5) The heat transfer coefficient becomes lower with the increment of salinity.

Acknowledgment

This research was supported by the project of Chinese National Natural Science Foundation (No. 51176017), the project of Shanghai Science and Technology Scheme (09DZ1200502) and Fundamental Research Funds for the Central Universities (DUT13RC(3)49). The authors are grateful for their financial support.

Nomenclature

D	—	tube diameter (mm)
T_{sat}	—	saturation temperature ($^{\circ}\text{C}$)
h	—	heat transfer coefficient ($\text{kW}/\text{m}^2\text{C}$)
F_a	—	heat transfer area (m^2)
η	—	viscosity
F_s	—	heat transfer area of single tube (m^2)
λ	—	thermal conductivity ($\text{W}/\text{m}^{\circ}\text{C}$)
S	—	salinity (g/kg)
Δt	—	temperature difference ($^{\circ}\text{C}$)
n	—	tube amount
Γ	—	spray density (kg/ms)
q	—	heat flux (kW/m^2)
Q_a	—	heat transfer capacity (kW)
v	—	velocity (m/s)
Φ	—	the coefficient for effective volume of the evaporators

Subscripts

tri	—	triangular pitch
rtri	—	rotated triangular pitch
squ	—	square pitch
rsqu	—	rotated square pitch

References

- [1] A.D. Khawaji, I.K. Kutubkhanah, Advances in seawater desalination technologies, *Desalination* 221 (2008) 47–69.
- [2] L. Xie, P. Li, S. Wang, A review of seawater desalination and comparison of desalting processes, *Chem. Ind. Eng. Progr.* 22(10) (2003) 1081–1084.
- [3] X. Zeng, M. Chyu, Z. Ayub, Experimental investigation on ammonia spray evaporator with triangular-pitch plain-tube bundle, Part I: Tube bundle effect, *Int. J. Heat Mass Transfer* 44 (2001) 2299–2310.
- [4] X. Zeng, M. Chyu, Z. Ayub, Experimental investigation on ammonia spray evaporator with triangular-pitch plain-tube bundle, Part II: Evaporator performance, *Int. J. Heat Mass Transfer* 44 (2001) 2081–2092.
- [5] S. Moeykens, M. Pate, Spray evaporation heat transfer of R-134a on plain tubes, *ASHRAE Trans.* 100(2) (1994) 173–184.
- [6] Z. Liu, J. Yi, Enhanced evaporation heat transfer of water and R-11 falling film with the roll-worked enhanced tube bundle, *Exp. Thermal Fluid Sci.* 25 (2001) 447–455.
- [7] G. Ribatski, A.M. Jacobi, Falling film evaporation on horizontal tubes—A critical review, *Int. J. Refrig.* 28 (2005) 635–653.
- [8] L. Yang, S. Shen, Experimental study of falling film evaporation heat transfer outside horizontal tubes, *Desalination* 220 (2008) 654–660.
- [9] G. Jelino, Pilot Plant Test and Design Study of a 2.5 MGD Horizontal-tube Multiple-effect plant, Office of Saline Water Research and Development Progress Report. No 492, 1969.
- [10] R. Bellman, R. Pennington, Effects of surface tension and viscosity on Taylor instability, *Quart. Appl. Math.* 12 (1954) 151–162.
- [11] X. Mu, S. Shen, Y. Yang, X. Liu, Experimental study of falling film evaporation heat transfer coefficient on horizontal tube, *Desalin. Water Treat.* 50 (2012) 310–316.
- [12] B. Fabuss, A. Korosi, OSWR&D Progress Report No 384, 1968
- [13] P. Zhang, Study on the surface tension of sea water, *J. Shanxi Normal Univ., Natural Sci. Ed.* 25(4) (2011) 44–45.
- [14] M.H. Sharqawy, J.H. Lienhard, S.M. Zubair, Thermophysical properties of seawater: a review of existing correlations and data, *Desalin. Water Treat.* 16 (2010) 354–380.